

Full Length Research Paper

Calculation of the electron drift mobility in $\text{Cr}^{2+}:\text{ZnS}$ and $\text{Cr}^{2+}:\text{ZnSe}$ materials by rode iteration model

H. Arabshahi

Physics Department, Ferdowsi University of Mashhad, Mashhad, Iran. E-mail: arabshahi@um.ac.ir.

Accepted 24 August, 2010

The results of electron drift velocity in $\text{Cr}^{2+}:\text{ZnS}$, and $\text{Cr}^{2+}:\text{ZnSe}$ are calculated for different temperature, free-electron concentrations and compositions. The two-mode nature of the polar optic phonons is considered jointly with deformation potential acoustic, piezoelectric, alloy and ionized-impurity scattering. Band non-parabolicity, admixture of p functions, arbitrary degeneracy of the electron distribution, and the screening effects of free carriers on the scattering probabilities are incorporated. The Boltzmann equation is solved by an iterative technique using the currently established values of the material parameters. The iterative results are in fair agreement with other recent calculations obtained using the relaxation-time approximation and experimental methods.

Key words: Boltzmann equation, electron drift velocity, deformation potential, piezoelectric.

INTRODUCTION

$\text{Cr}^{2+}:\text{ZnS}$, and $\text{Cr}^{2+}:\text{ZnSe}$ saturable absorbers are ideal materials for passive Q-switches of eye-safe fiber and solid-state lasers operating in the spectral range of 1.5 - 2.1 μm . These lasers are used in numerous applications, such as free-space communication systems, target designation, time-of-flight range finding, surgery, reflectometry, laser lidars, etc. Recently manufacturer offers a large variety of diffusion-doped $\text{Cr}^{2+}:\text{ZnS}$, and $\text{Cr}^{2+}:\text{ZnSe}$ polycrystals appropriate for Q-switching of the lasers operating in the 1.5 - 2.1 μm spectral range (Bhaskar et al., 1997). Recently, there has been considerable interest in the electron transport in submicron $\text{Cr}^{2+}:\text{ZnS}$, and $\text{Cr}^{2+}:\text{ZnSe}$ for possible high-frequency and high-speed applications. As the transit time of electrons in a device becomes comparable, or less than, the mean free time between collisions, the electrons will move more or less ballistically in the device, and will obtain very high velocities (Besikci et al., 2000). Simulations of these phenomena in a diode structure have so far only been carried out for a very small anode voltage, or with rather artificial cathode and anode structures (Izuka and Fukuma, 1990). However, simulations for higher anode voltages are needed in view of the situation in practical devices where engineering problems call for anode voltages of no less than about the Schottky barrier height or the p-n junction barrier height (Besikci et

al., 2000). The boundary conditions are important as they have significant influence on the space-charge-limited current flow which becomes dominant in submicron devices. In this paper we report a Rode iteration model for calculation of electron transport in a submicron $\text{Cr}^{2+}:\text{ZnS}$, and $\text{Cr}^{2+}:\text{ZnSe}$ materials.

In $\text{Cr}^{2+}:\text{ZnS}$, and $\text{Cr}^{2+}:\text{ZnSe}$ compounds the dominant scattering mechanisms is primarily the polar optic phonon scattering mechanism. The others are ionized impurity scattering, acoustic phonon deformation potential scattering and acoustic phonon piezoelectric scattering mechanisms. As a result of being elastic process of acoustic phonon deformation potential scattering, acoustic piezoelectric scattering and ionized impurity scattering, their mobilities can be calculated with the relaxation time approach. But if the electron energy can be compared with the phonon energy, this is important and such a scattering is inelastic scattering. The compensated changing in the energy is taken place after inelastic scattering. Since in inelastic scattering process the phonon energy is the bigger than the electron energy. Thus, relaxation time approach is not valid for inelastic scattering process. Because of this the calculation of polar optic phonon scattering is used the other numerical method instead of relaxation time approach. In this work it was used an iterative method for the calculation.

THEORETICAL MODEL

In principle the iterative technique give exact numerical prediction of electron mobility in bulk semiconductors. To calculate mobility, we have to solve the Boltzmann equation to get the modified probability distribution function under the action of a steady electric field. Here, we have adopted the iterative technique for solving the Boltzmann transport equation. The electron distribution function $f(k)$ in the presence of an electric field E is expressed as:

$$f(k) = f_0(E) + \left[\frac{e\hbar E}{m^*} \right] k \varphi(k) \times \left(\frac{\partial f_0}{\partial E} \right) \cos \theta \quad (1)$$

where $f_0(E)$ is the thermal equilibrium Fermi-Dirac distribution function, e is the magnitude of the electron charge, θ is the angle between k and E and $\varphi(E)$ is the perturbation function to be determined from the Boltzmann equation. The Boltzmann equation for electrons, with Fermi-Dirac statistics, describes classical transport phenomena with which we are presently concerned exclusively. Allowing for an electric field E and a spatial gradient parallel to E , we have Mogilestue (1993).

$$v \cdot \nabla_T + \frac{e}{\hbar} E \cdot \nabla_k f_k = \int [s' f'(T)(1-f(T)) - s f_T(1-f'(T))] d^3 k \quad (2)$$

where $f'_T = f_T(k')$, $s = s(k, k')$ and $s' = s(k', k)$ is the differential scattering rate for an electron in the state characterized by k' to make a transition into the state characterized by k . Substitution of Equation 1 into Equation 2 and integration over all final states and considering all differential scattering rates, the factor $\varphi(k)$ in the perturbed part of the distribution function $f(k)$ can be given by Jacoboni et al. (1989).

$$\varphi(k) = \frac{-eF \frac{\partial f_0}{\partial k} + \sum \int f_1' \cos \varphi [s_{inel}'(1-f_0) + s_{inel} f_0] d^3 k'}{\sum \int (1 - \cos \varphi) s_{el} d^3 k' + \sum \int [s_{inel}(1-f_0') + s_{inel}' f_0'] d^3 k'} \quad (3)$$

The symbol sel and s_{inel} denotes the sum of both the scattering-out and scattering-in rates for all the elastic scattering processes, namely, deformation-potential acoustic, piezoelectric, alloy and ionized impurity modes of scattering and inelastic scattering processes like polar optic mode. All the relevant expressions, except for alloy scattering, including non-parabolicity, p -function admixture, arbitrary degeneracy of the electron distribution, and the screening effects of the free carriers, are well known. The expression for alloy scattering, incorporating the same effects, is developed following Arabshahi et al. (2008).

Equation 3 is solved for $\varphi(k)$ by the numerical iterative method. Note, the first term in the denominator is simply the momentum relaxation rate for elastic scattering. It is interesting to note that if the initial distribution is chosen to be the equilibrium distribution, for which $\varphi(k)$ is equal zero, we get the relaxation time approximation result after the first iteration. We have found that convergence can normally be achieved after only a few iterations for small electric fields. Once $\varphi(k)$ has been evaluated to the required accuracy, it is possible to calculate quantities such as the electron drift mobility which is given by;

$$\mu = \frac{\hbar}{3m^* F} \frac{\int_0^\infty (k^3 / 1 + 2\alpha F) f_1 d^3 k}{\int_0^\infty k^2 f_0 d^3 k} \quad (4)$$

Here, we have calculated low field drift mobility in $\text{Cr}^{2+}:\text{ZnS}$, and $\text{Cr}^{2+}:\text{ZnSe}$ materials using the iterative technique. The effects of piezoelectric, acoustic deformation, polar optical phonons and ionized impurity scattering have been included in the model. It is also assumed that the electrons remain in the Γ -valley of the Brillouin zone. Further we supposed that the materials have the isotropic non parabolic band structure. We took into account electron screening and mixing of s and p wave functions.

RESULTS

Calculation results in $\text{Cr}^{2+}:\text{ZnS}$, and $\text{Cr}^{2+}:\text{ZnSe}$

Figure 1 shows the temperature dependence of electron drift mobility in $\text{Cr}^{2+}:\text{ZnS}$, and $\text{Cr}^{2+}:\text{ZnSe}$. The electron drift mobilities at room temperature that we find are 900 and 700 $\text{cm}^2 \text{V}^{-1} \text{s}^{-1}$ for $\text{Cr}^{2+}:\text{ZnSe}$ and $\text{Cr}^{2+}:\text{ZnS}$ structures, respectively, for an electric field equal to 10^4 Vm^{-1} and with a donor concentration of 10^{22} m^{-3} . The material parameters used to calculate the electron drift mobilities are tabulated in Table 1. The results plotted in Figure 1 indicate that the electron drift mobility of $\text{Cr}^{2+}:\text{ZnS}$ is lower than that for the $\text{Cr}^{2+}:\text{ZnSe}$ structure. This is largely due to the higher Γ valley effective mass in the $\text{Cr}^{2+}:\text{ZnS}$ structure.

Figure 2 shows the calculated variation of the electron mobility as a function of the donor concentration for both $\text{Cr}^{2+}:\text{ZnS}$ and $\text{Cr}^{2+}:\text{ZnSe}$ crystal structures at room temperature. The mobility does not vary monotonically between donor concentrations of 10^{22} and 10^{23} m^{-3} due to the dependence of electron scattering on donor concentration, but shows a maximum at 10^{22} m^{-3} for both compounds. In order to understand the scattering mechanisms which limit the mobility of $\text{Cr}^{2+}:\text{ZnSe}$ and $\text{Cr}^{2+}:\text{ZnS}$ under various conditions, we have performed calculations of the electron drift mobility when particular scattering processes are ignored. The solid circle curve in Figure 3 shows the calculated mobility for $\text{Cr}^{2+}:\text{ZnS}$ material including all scattering mechanisms whereas the open circle and star curves show the calculated mobility without ionized impurity and polar optical scattering, respectively. It can be seen that below 200 K the ionized impurity scattering is dominant while at the higher temperatures electron scattering is predominantly by optical modes. Thus the marked reduction in mobility at low temperatures seen in Figure 3 can be ascribed to impurity scattering and that at high temperatures to polar optical phonon scattering. The temperature variation of the electron drift mobility in $\text{Cr}^{2+}:\text{ZnSe}$ and $\text{Cr}^{2+}:\text{ZnS}$ compounds for different donor concentrations is shown in Figure 4. It is evident from this figure that the curves approach each other at very high temperatures, where the mobility is limited by longitudinal optical phonon scattering, whereas the mobility varies inversely with donor concentration at low temperatures as we would expect from the foregoing discussion.

Conclusions

In conclusion, we have studied the electron transport

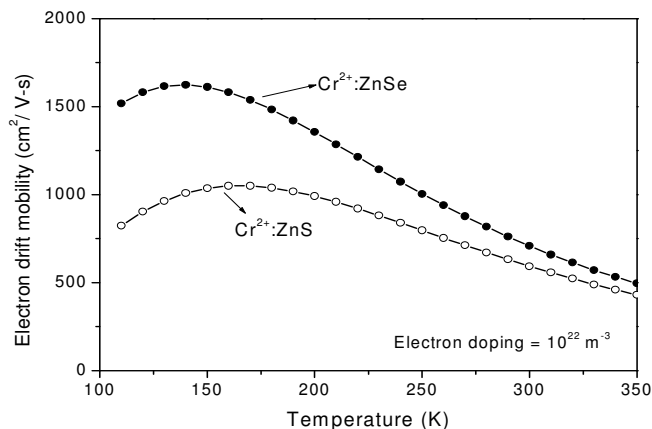


Figure 1. Electron drift mobility of $\text{Cr}^{2+}:\text{ZnS}$ and $\text{Cr}^{2+}:\text{ZnSe}$ structures versus temperature. Donor concentration is approximately 10^{22} m^{-3} .

Table 1. Important parameters used in our calculations for $\text{Cr}^{2+}:\text{ZnS}$, and $\text{Cr}^{2+}:\text{ZnSe}$ materials which are taken from references.

Parameter	$\text{Cr}^{2+}:\text{ZnS}$	$\text{Cr}^{2+}:\text{ZnSe}$
Density ρ (kgm^{-3})	4015	5210
Longitudinal sound velocity v_s (ms^{-1})	564686	4640
Low-frequency dielectric constant ϵ_s	9.2	9
High-frequency dielectric constant ϵ_∞	5.3	14.2
Acoustic deformation potential (eV)	4.5	3.4
Polar optical phonon energy (eV)	0.0366	0.03
Γ -valley effective mass (m)	0.25	0.15
Γ -valley non parabolicity (eV^{-1})	0.6	0.53

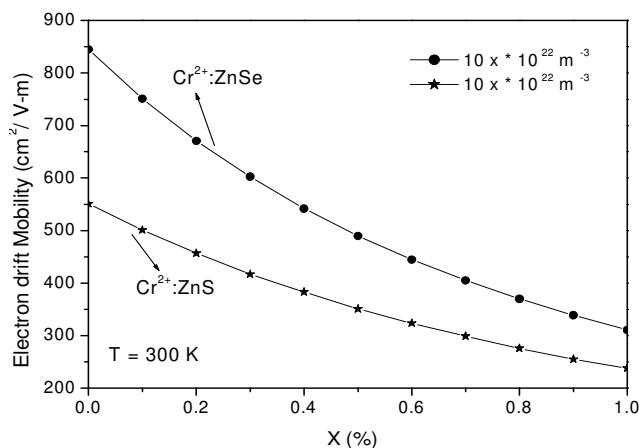


Figure 2. Electron drift mobility of $\text{Cr}^{2+}:\text{ZnS}$ and $\text{Cr}^{2+}:\text{ZnSe}$ structures versus donor concentration at room temperature.

characteristic associated with $\text{Cr}^{2+}:\text{ZnSe}$ and $\text{Cr}^{2+}:\text{ZnS}$ compounds. The details of band structure and scattering mechanisms are included without applying Matthiessen's

rule. Temperature dependent and free electron concentration dependent of the electron mobility in both structures have been compared. It has been found that

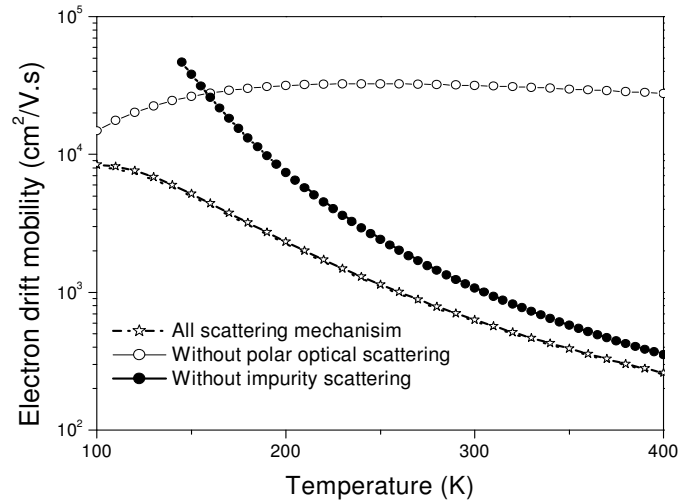


Figure 3. Comparison of electron drift mobility $\text{Cr}^{2+}:\text{ZnS}$ material with donor concentration of 10^{22} m^{-3} and when individual scattering processes are ignored.

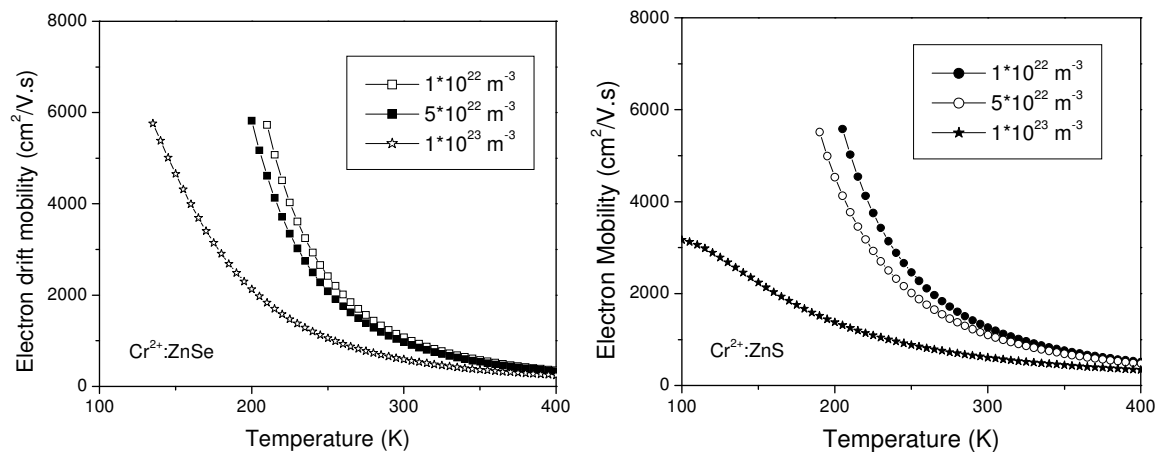


Figure 4. Calculated low-field electron drift mobility of $\text{Cr}^{2+}:\text{ZnS}$ and $\text{Cr}^{2+}:\text{ZnSe}$ compounds as functions of temperature for different donor concentrations.

$\text{Cr}^{2+}:\text{ZnSe}$ and $\text{Cr}^{2+}:\text{ZnS}$ structure due to the lower electron effective mass in this crystal structure. Ionized impurities have been treated beyond the born approximation using a phase shift analysis. Screening of ionized impurities has been treated more realistically using a multi-ion screening formalism, which is more relevant in the case of highly compensated III-V semiconductors.

ACKNOWLEDGEMENT

The author would like to thank Maryam Gholvani for writing up the paper.

REFERENCES

- Arabshahi H, Khalvati MR, Rezaee, Rokn-Abadi M (2008). Monte Carlo modeling of hot electron transport in bulk AlAs, AlGaAs and GaAs at room temperature. *Modern Phys.Lett.*, 22 (18): 1777-1784.
- Besikci B, Bakir M, Tanatar U (2000). Hot electron simulation devices. *J. Appl. Phys.*, 88(3): 1243-1247.
- Bhaskar UV, Shur MS (1997). Ensemble Monte Carlo study of electron transport in wurtzite InN. *J. Appl. Phys.*, 82: 1649-1654.
- Izuka J, Fukuma M (1990). Full-band polar optical phonon scattering analysis and negative differential conductivity in wurtzite GaN. *Solid-State Electron*, 3: 27-33.
- Jacoboni J, Lugli P (1989). *The Monte Carlo method for semiconductor and device simulation*. Springer-Verlag.